J Membrane Biol (2013) 246:697–704
DOI 10.1007/s00232-013-9587-y

Carbon Nanotube-Encapsulated Drug Penetration Through the Cell Membrane: An Investigation Based on Steered Molecular Dynamics Simulation

Seyedeh Zahra Mousavi · Sepideh Amjad-Iranagh · Yousef Nademi · Hamid Modarress

Received: 17 March 2013 / Accepted: 8 August 2013 / Published online: 25 August 2013

Abstract Understanding the penetration mechanisms of carbon nanotube (CNTs)-encapsulated drugs through the phospholipid bilayer cell membrane is an important issue for the development of intracellular drug delivery systems. In the present work, steered molecular dynamics (SMD) simulation was used to explore the possibility of penetration of a polar drug, paclitaxel (PTX), encapsulated inside the CNT, through a dipalmitoylphosphatidylcholine bilayer membrane. The interactions between PTX and CNT and between PTX and the confined water molecules inside the CNT had a significant effect on the penetration process of PTX. The results reveal that the presence of a PTX molecule increases the magnitude of the pulling force. The effect of pulling velocity on the penetration mechanism was also investigated by a series of SMD simulations, and it is shown that the pulling velocity had a significant effect on pulling force and the interaction between lipid bilayer and drug molecule.

Keywords Carbon nanotube · Paclitaxel · Lipid bilayer · Drug delivery

Electronic supplementary material The online version of this article (doi:10.1007/s00232-013-9587-y) contains supplementary material, which is available to authorized users.

S. Z. Mousavi · S. Amjad-Iranagh · Y. Nademi · H. Modarress (✉)
Department of Chemical Engineering, Amirkabir University of Technology, Hafez Avenue, Tehran, Iran
e-mail: hmodares@aut.ac.ir

S. Amjad-Iranagh
Department of Chemistry, Amirkabir University of Technology, Hafez Avenue, Tehran, Iran

Introduction

Progress in the medical research has resulted in the generation of new synthetic drugs. The optimized action of these drugs is related to their achievement of the target organism and transmission through the biological membranes. The cell membrane, as a protective barrier to the external molecules, does not permit drug molecules to enter the cell. Most drug molecules are polar and have complicated structures, which cause difficulties in their transmission through the cell membrane. However, the probability of targeted transmission will increase with drug delivery devices (Farokhzad and Langer 2009; Surendiran et al. 2009). These drug delivery devices are loaded with lower doses of drug cargo, can minimize the side effects of toxic drugs and can increase treatment efficiency (Hughes 2005; Ulbrich and Lamprecht 2010). Nanocarriers or nanocapsules are such drug delivery devices (Ochekpe et al. 2009). Among these nanocarriers carbon nanotubes (CNTs) have a special place, due to their unique properties, such as the ability to interact with biological molecules (Jana et al. 2013; Zuo et al. 2010, 2011) and to enter the cell nuclei (Martin and Kohli 2003; Pantaotto et al. 2004), large inner volume (Faraji and Wipf 2009), good biocompatibility (Ochekpe et al. 2009) and high aspect ratio (Bianco et al. 2005). Observations of single-wall nanotube penetration into the cell by electron microscopy (Porter et al. 2007), spectroscopy (Khodakovskaya et al. 2009) and fluorescent microscopy (Cherukuri et al. 2004) have shown that the CNT can easily enter the cell. This property is useful for the delivery of anticancer (Lay et al. 2010; Liu et al. 2008; Shuai et al. 2010), antibacterial and anti-inflammatory (Sung et al. 2009) agents into the cell. These compounds are attached to the surface of the CNT via covalent bonding (DeVane et al. 2008; Liu et al. 2008;

Shuai et al. 2010; Sung et al. 2009), noncovalent coating (Dhar et al. 2008) and physical functionalization (Cherukuri et al. 2004). The cargo can also be encapsulated inside the large volume of the CNT (Panczyk and Warzocha 2009). It seems that encapsulation is a better method because the drug agent is kept in a defended environment that cannot be destroyed by enzymes (Chaban et al. 2010). Both theoretical and experimental studies have shown that loading of drug molecule and its unloading after entering the cell is possible (Hari et al. 2006; Hilder and Hill 2008a, 2008b; Kang et al. 2008; Su et al. 2011). Although experiments provide information about the CNT, as a drug delivery device, its cargo and its diffusion through the membrane, it is useful to use molecular dynamics (MD) simulation to explore the effective interactions at the single-molecule level (Jana et al. 2013; Johnson et al. 2009; Lee 2013).

MD has already been applied to other CNT–drug or CNT–membrane systems. A group of simulations, related to drug release, has used near-infrared radiation (Chaban et al. 2010), magnetic field (Panczyk et al. 2010; Panczyk and Warzocha 2009) and a chemical trigger like pH (LaVan et al. 2003) as driving forces for the release of the drug cargo from the CNT. Another group of simulations has studied the interaction of the CNT with the cell membrane (DeVane et al. 2008; Gangupomu and Capaldi 2011; Wallace and Sansom 2008).

In the present work, we studied a step after the drug encapsulation and before its release that is the penetration of the encapsulated drug into the inner space of the CNT across the cell membrane. However, the diffusion process is very slow and difficult to perform with the MD timescale, so it should be accelerated (Izrailev et al. 1997; Kang et al. 2008); and a series of steered molecular dynamics (SMD) simulations were performed. The purpose of this study was to explore the conformational change of the dipalmitoylphosphatidylcholine (DPPC) bilayer membrane as a result of interaction with CNT encapsulating a drug and the confined water molecules and to examine to what extent the drug and pulling force could affect the penetration process into the membrane. Paclitaxel (PTX) as a sample drug is used, which is known as an anticancer drug and has a polar core (Snyder et al. 2001). The structure of PTX is shown in Fig. 1. The simulation results support the idea that use of the CNT facilitates the targeted penetration of the polar drugs into the biological cell and produces informative details of the penetration process.

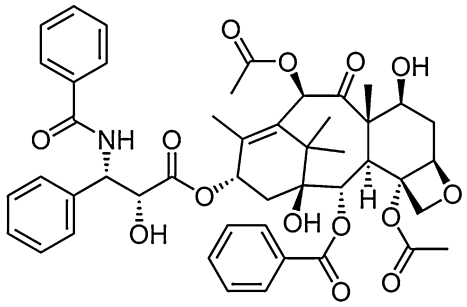

Fig. 1 Structure of PTX, combining a polar and rigid tetracyclic core with an equally polar set of four flexible side chains (Snyder et al. 2001)

Computational Methods

Force Fields

The GROMACS 4.5.4 program (Hess et al. 2008) was used to perform all simulations, and PyMOL (v. 1.4.1) was used for visualization (DeLano 2002). The all-atom GROMOS43A1 force field (van Gunsteren et al. 1996) was employed to calculate all bonded and nonbonded interactions. Lorenz-Berthelot combination rules were used to obtain the cross-term Lennard-Jones (12, 6) parameters (Allen and Tildesley 1987), and the graphite parameters were used to supplement that of the CNT (Walther et al. 2001). Water molecules are modeled as a simple point charge, which is usually used for all GROMOS force fields (Berendsen et al. 1981).

The simulation system consisted of 384 DPPC molecules, a single-wall CNT and a PTX molecule. The DPPC bilayer was previously equilibrated at 323 K (Domanski et al. 2010). The (15,15) single-wall CNT with a diameter of about 1.0 nm and length of 5.0 nm was built using a visual MD program (Humphrey et al. 1996). This nanotube is appropriate for efficient encapsulation of PTX (Hilder and Hill 2008b). The PTX topology files corresponding to the current force field were prepared using the PRODRG server (Schuttelkopf and van Aalten 2004), and then it was optimized by the AM1 semiempirical method of HyperChem software (v. 7). One of the simulation systems consisted of the CNT and DPPC molecules, but the other systems consisted of the CNT, PTX and DPPC.

Simulation Details

The simulations were run in the NPT ensemble, which is known as a favorable ensemble for membrane simulations (Egberts et al. 1994; Gangupomu and Capaldi 2011; Shepherd et al. 2001; Tieleman et al. 1997; Wallace and Sansom 2008). During the simulation the temperature was kept constant at 323 K using a Nosé-Hoover thermostat (Hoover 1985), and the pressure was kept constant at 1 bar using the Parrinello–Rahman barostat (Parrinello and Rahman 1980) with semi-isotropic pressure coupling, which is appropriate for membrane protein simulation (Kandt et al. 2007). The time step was 2fs, and the LINCS algorithm (Hess et al. 1997) was used to constrain all

bonds. The long-range electrostatic interaction was calculated with the particle mesh Ewald method (Darden et al. 1993) with a cutoff radius of 1.0 nm. The Lennard-Jones potential was used to calculate the van der Waals interaction with a cutoff radius of 1.4 nm as recommended (Sutmann 2002).

The simulation cell was constructed with the dimensions of 114 × 114 × 260 Å^3. The CNT was initially at a distance of 1.0 nm from the DPPC membrane. The PTX molecule was located inside the CNT to represent the loaded CNT without any constraint. The system was solvated with 91,475 water molecules, as shown in Fig. 2; then, the energy was minimized using the steepest descent method. During 6.5 ns of an equilibration run, where the CNT was constrained, PTX, membrane and water molecules were equilibrated. After the equilibration, the area per lipid was calculated and a value of 64.0 Å^2 was obtained, which is in agreement with the experimental measurements (Nagle 1993). Following the equilibration, constant velocity SMD was used. In SMD simulation, the CNT and the encapsulated PTX were attached to dummy atoms via a virtual spring and were moved at a constant velocity. The force needed for the displacement of the dummy atoms to an imaginary point can be calculated by the following equations:

$$F = -\nabla U \tag{1}$$

$$U = \frac{1}{2}k[vt - (r - r_0) \cdot n]^2 \tag{2}$$

where ∇U is the potential energy gradient, k is the spring force constant, v is the velocity of pulling, t is the current time, r is the instantaneous vector position, r_0 is the initial vector position of the SMD atom and n is the vector direction which the dummy atom is pulled.

In the SMD simulation of the present work, four pulling velocities (v) in the range of 0.1–0.025 Å/ps were used and each simulation was repeated to confirm the results. The CNT was restrained by the same force constant in the x and y directions and pulled in the z direction perpendicular to the membrane plane. The required pulling force is the smallest when the CNTs penetrate perpendicularly rather than obliquely or parallel to the membrane (Gangupomu and Capaldi 2011; Wallace and Sansom 2008), and since perpendicular diffusion was observed experimentally, this direction of pulling seems logical (DeVane et al. 2008; Gangupomu and Capaldi 2011; Shi et al. 2008).

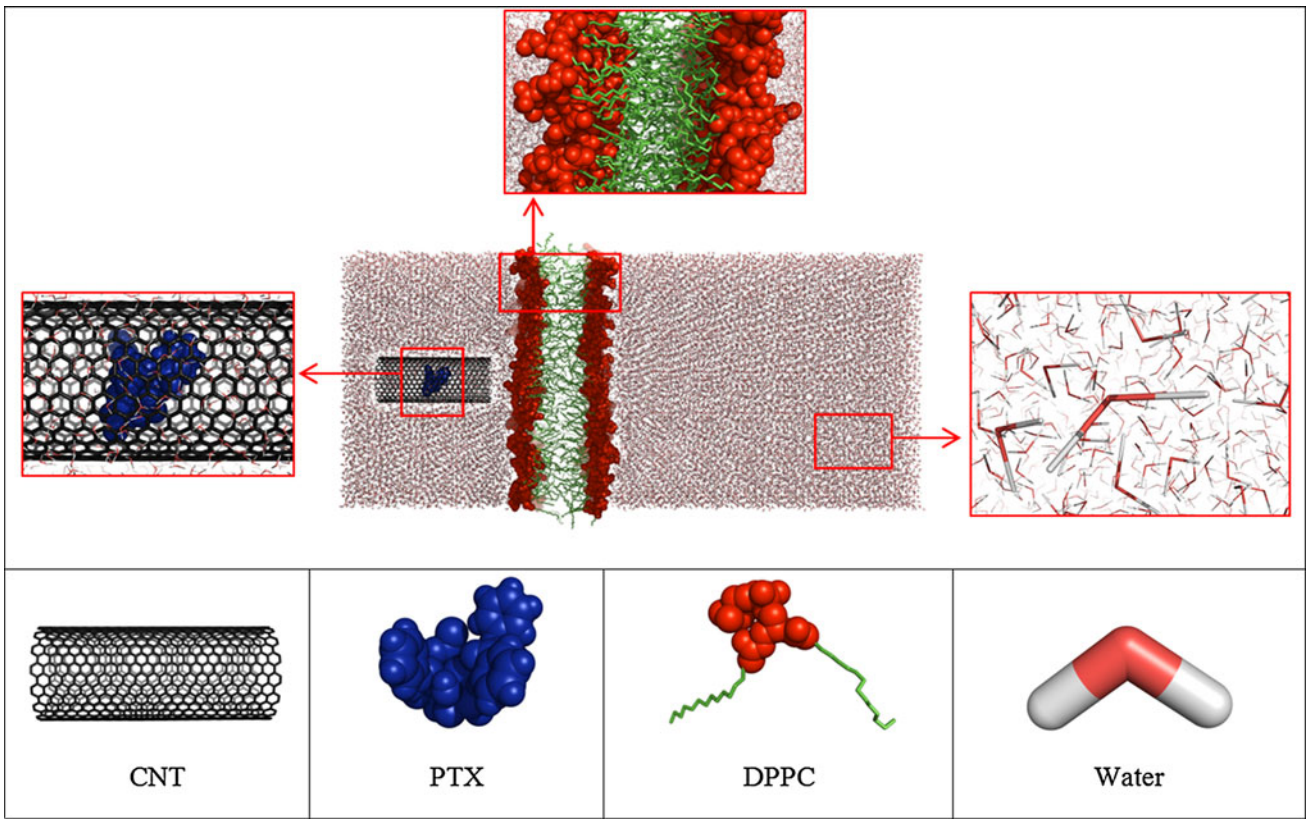

Fig. 2 The solvated system: the simulation cell has the dimensions 114 × 114 × 260 Å^3, the CNT is at a distance of 1.0 nm from the DPPC membrane and the PTX molecule is located inside the CNT. The hydrophilic DPPC head-group particles are shown in *red*, while the hydrophobic tail particles are shown in *green*, the CNT is shown in *black* and PTX is shown in *blue*. The molecular structures of CNT, PTX, DPPC and water are also shown separately. (Color figure online)

Results and Discussion

CNT Penetration Mechanism

Initially, the CNT-encapsulated PTX was positioned at a distance of 1.0 nm from the lipid bilayer membrane (Fig. 3a) and pulled with a velocity of 0.1 Å/ps and a spring constant of 10 kJ mol^{-1} $Å^{-2}$. Then, the CNT was moved closer to the membrane (Fig. 3b) until it reached the membrane surface, and as a result the membrane was perturbed and a curvature appeared on its surface. The high velocity of the CNT gives a concave shape to the upper leaflet of the bilayer membrane surface (Fig. 3c). During the exiting process of the CNT, the pulling velocity gave a convex shape to the lower bilayer leaflet, as shown in Fig. 3d. When the CNT was pulled to exit the center of the DPPC lipid bilayer, a hydrophobic mismatch between the CNT and the lipid molecules was observed, so the lipid

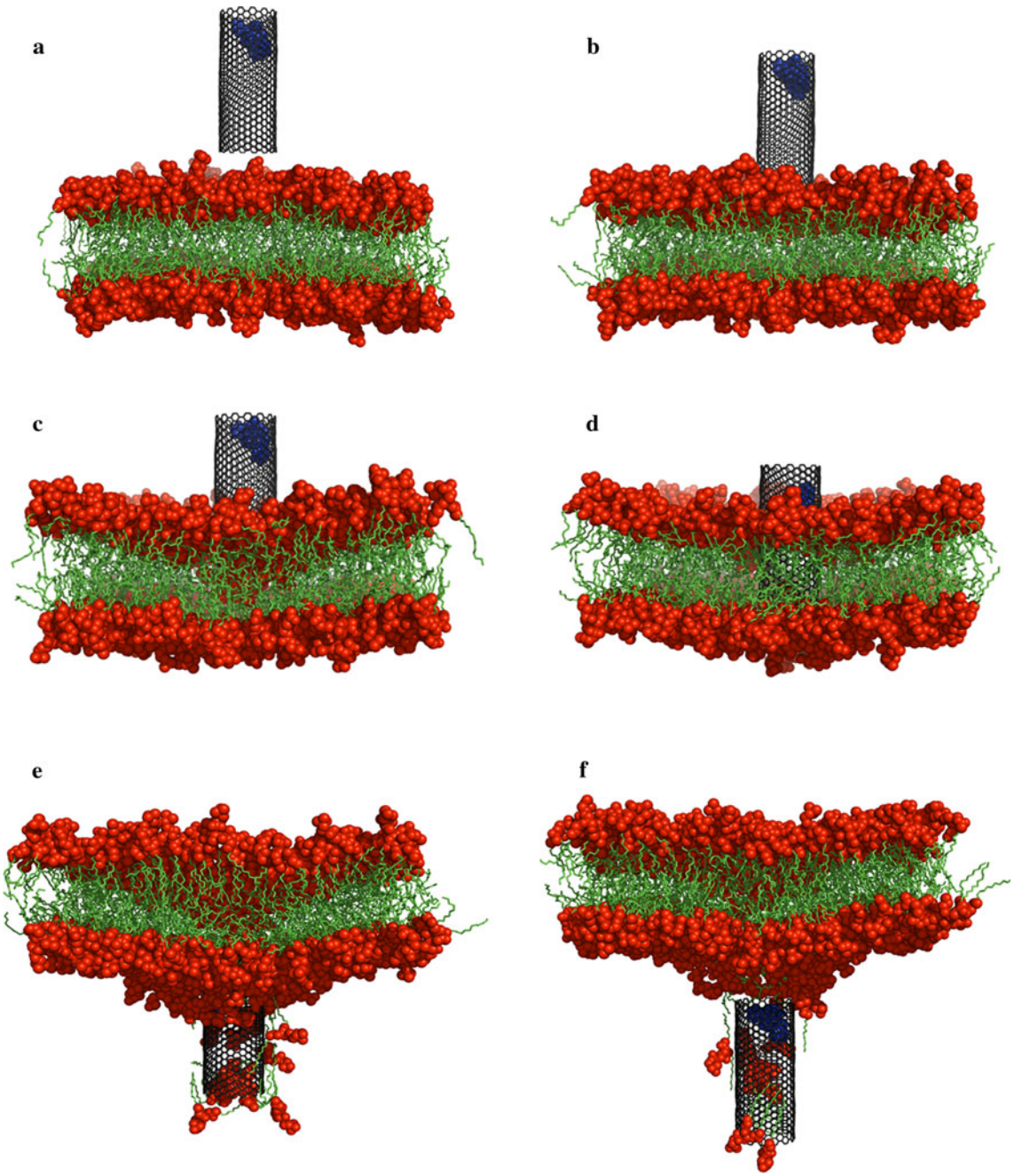

Fig. 3 Snapshots of CNT–PTX penetration through the lipid bilayer. Water molecules are eliminated to clarify the snapshots. The color scheme is the same as that used in Fig. 2

tails, surrounding the tube, were stretched and wrapped the outer surface of the CNT to minimize unfavorable exposure of the hydrophobic core to the aqueous environment (Fig. 3e). Finally, when the CNT exited the membrane, some lipids were extracted with it; these lipid molecules were inside or on the outer surface of the CNT (Fig. 3f).

It is useful to see the force–displacement curve, which is plotted in Fig. 4. During the simulation, the velocity was constant and the instantaneous vector position of the drug delivery system changed with time, so if this vector increases with time, the displacement $(r - r_0)$ would increase and, as a consequence, the potential energy would decrease according to Eq. (2). The reduction of the pulling force is the result of this situation (Eq. 1), and it shows that the system does not resist moving so much. As observed in Fig. 4, initially, when the CNT is pulled to traverse the hydrophilic phase of the bilayer (at an interval of about 0–35 Å), the required force for pulling becomes higher because CNT prevents entering a hydrophilic phase; hence, the instantaneous position of the CNT does not change so much with time, and this causes an increase in the force. Besides, some lipid molecules extend and move upward to wrap the CNT from the aqueous environment. These movements cause an increase in the force since the lipids exert an extra force on the CNT. This increase of force will continue until a noticeable part of the CNT enters the hydrophobic phase of the lipid bilayer. After that, once the CNT penetrates more (at an interval of about 35–60 Å), the force magnitude decreases because the hydrophobic CNT is in the hydrophobic phase of the bilayer and, as a consequence, the resistance decreases against its movements and its energy decreases. Reduction of the Lennard-Jones potential as a result of the CNT and DPPC lipid molecule interaction in this interval, which is shown in Fig. 5, confirms this viewpoint. Again, when the CNT is pulled to leave the hydrophobic lipid tails and approaches the hydrophilic lipid head groups (at an interval of about 60–100 Å), the applied force increases since the lipids exert an extra force on the CNT to pull it into the bilayer core. Finally, when the CNT exits the bilayer, some lipids which are extracted shield the outer surface of the CNT and prevent it from encountering water molecules; this phenomenon is shown in Fig. 3e.

It is useful to compare the profiles of the applied forces for the CNT-encapsulated PTX and CNT alone, as shown in Fig. 6. It is observed that the maximum and minimum of the two curves occur in the same displacement because the CNT, as a drug carrier, determines the shape of the force profile. But when the CNT is used as a drug carrier, the pulling force increases.

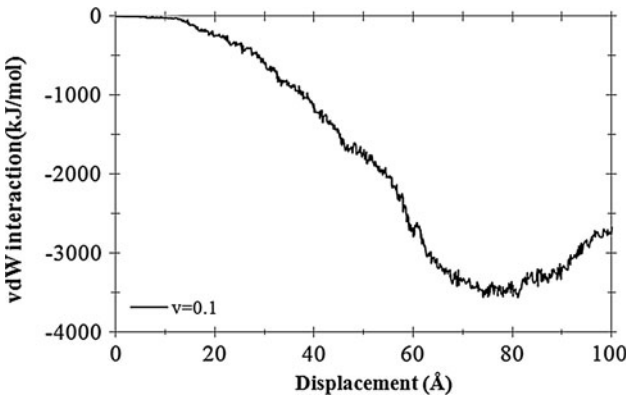

Fig. 5 van der Waals (*vdW*) interaction between CNT and DPPC lipid molecules versus displacement during the simulation. The interactions continue due to the extraction of some lipid molecules with CNT, although the drug-delivery system has exited the DPPC membrane

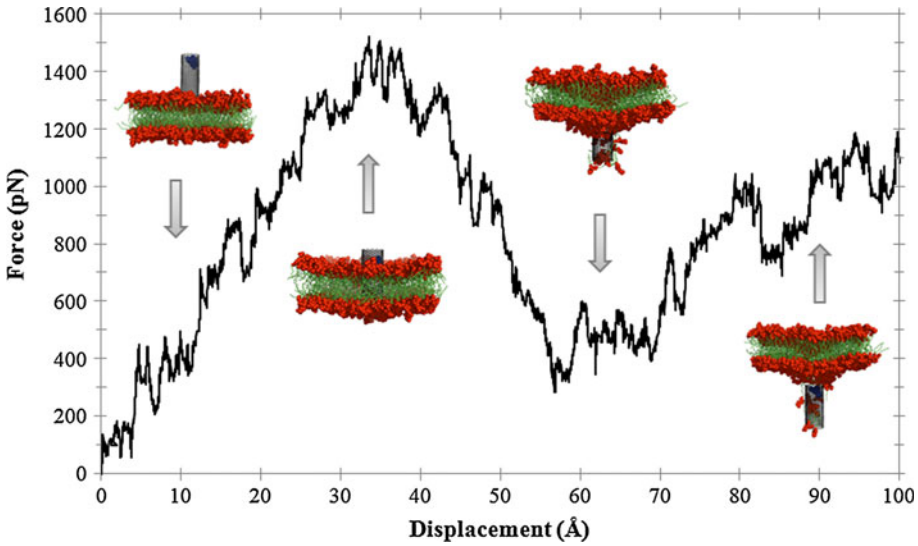

Fig. 4 The force–displacement profile of CNT and encapsulated PTX during the penetration at $v = 0.1$ Å/ps. *Displacement* refers to the distance between the instantaneous and the initial positions of the CNT encapsulated PTX. Different snapshots of the penetration mechanism were added in 10, 35, 65 and 90 Å. The color scheme is the same as that used in Fig. 2

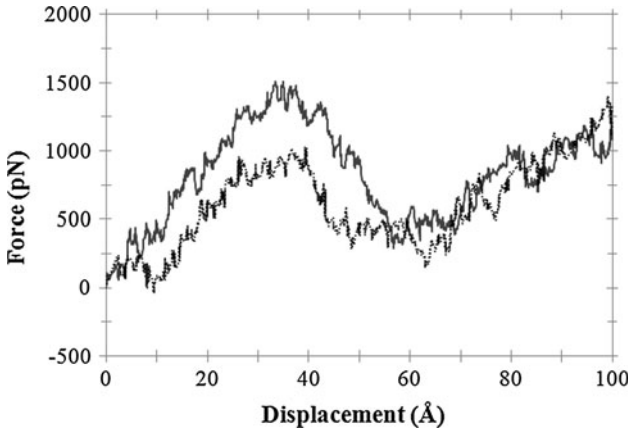

Fig. 6 The force–displacement profile of CNT and encapsulated PTX (*solid line*) and CNT (*dotted line*) during the penetration at $v = 0.1$ Å/ps. The profiles have the same shape

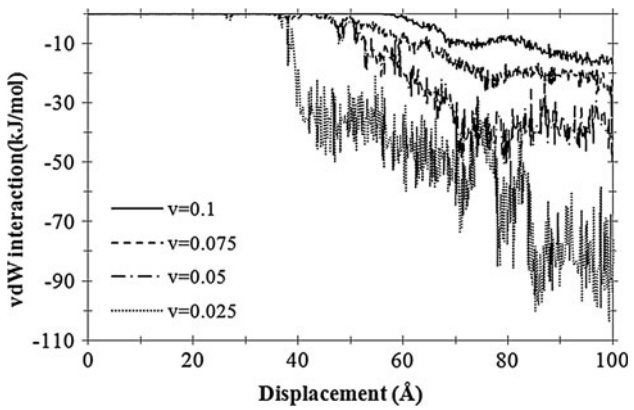

Fig. 7 van der Waals (*vdW*) interaction between encapsulated PTX and DPPC lipid molecules versus displacement during the simulation. The interactions start with a delay and continue due to the entrance of some lipid molecules into the CNT cavity, although the drug-delivery system exits the membrane

PTX Penetration Mechanism

Once the terminal part of the CNT penetrates into the membrane, the PTX molecule enters the bilayer and the van der Waals interaction between PTX and DPPC lipid molecules begins. As shown in Fig. 7, the interaction starts with a delay. During the transmission process some lipid molecules enter the interior cavity of the CNT; hence, this interaction will continue although the CNT has left the membrane (at a displacement of 100 Å). The number of DPPC molecules that enter the inner space of the CNT is listed in Table 1; the strength of this interaction depends on the number of these molecules, and the graphs of Fig. 7 confirm this viewpoint.

It was observed that the CNT and PTX van der Waals interaction was significant over the penetration mechanism (see details in Online Resource, Fig. S1). This interaction

Table 1 Number of DPPC lipid molecules that enter the interior cavity, number of extracted DPPC lipid molecules that exit with the CNT and average number of hydrogen bonds formed between PTX and the confined water molecules inside the CNT cavity during the simulation

Velocity (Å/ps)	Number of DPPC molecules that enter the CNT cavity	Number of extracted DPPC molecules with CNT	Number of hydrogen bonds
0.1	4	20	7.4
0.075	5	22	7.2
0.05	7	23	5.4
0.025	9	25	4.6

keeps PTX inside the CNT cavity during the transmission process across the lipid bilayer. Besides that, polar PTX prefers to stay hydrated by the interaction with water molecules and avoids entering the hydrophobic part of the lipid bilayer. The confined water molecules inside the cavity of the CNT provide such a suitable environment for the PTX, so it interacts with water molecules by hydrogen bond formation during the penetration process. The average number of hydrogen bonds which are formed between PTX and the confined water molecules inside the CNT cavity is listed in Table 1.

As reported in the previous simulation studies (Gangupomu and Capaldi 2011; Wallace and Sansom 2008), in the case of empty CNT, it was observed that its pore is completely filled with DPPC lipid molecules; and this confirms the disruption of the membrane. Also from these results it can be concluded that CNT has the dominant effect on the membrane disruption, whether or not the drug is present inside the CNT (see Online Resource, Fig. S2).

Effect of Pulling Velocity on Penetration Mechanism

In order to explore the influence of pulling rate on the penetration mechanism of the encapsulated PTX into the CNT, four different simulations have been implemented, with velocities of 0.1, 0.075, 0.05 and 0.025 Å/ps. As observed in the Online Resource, Fig. S3, in all the velocities the magnitude of the force increases as the CNT enters and exits the bilayer; upon reducing the pulling velocity, the pulling force reduces. Reduction of the required pulling force indicates that CNT and DPPC lipid molecules have more time to find the configuration with lower energy during the penetration process.

At low pulling velocities of CNT penetration into the lipid bilayer membrane the lipid molecules will have time to diffuse into the CNT cavity and replace the water molecules in the CNT cavity. Therefore, on reducing the number of water molecules in the CNT the number of

water molecules interacting with PTX will decrease. This is indicated clearly by the reduction of the number of hydrogen bonds between PTX and water molecules, as shown in Table 1.

According to Fig. 7, the strength of the interaction between DPPC lipid molecules and encapsulated PTX increases as the velocity decreases because of DPPC diffusion into the CNT cavity, as shown in Table 1. But the attractive forces between PTX and the CNT, which were almost the same in all the simulations, prevent the PTX molecule from being extracted from the interior cavity of the CNT when the lipid molecules enter the cavity of the CNT. However, by considering the interactions it can be predicted that the drug can traverse the bilayer with the help of the CNT, even at low velocities.

Conclusion

SMD simulations were used to explore the penetration of encapsulated PTX into the CNT, through the phospholipid bilayer membrane. It has been shown that the CNT facilitates targeted delivery of the polar PTX molecule through the lipid bilayer since it has the ability to penetrate into the cell membrane. The van der Waals interaction between PTX and the CNT, in addition to the hydrogen bond formation of PTX with the confined water molecules inside the CNT, plays an important role in the delivery of PTX as a drug. The effect of pulling rate on the penetration of the encapsulated PTX in the CNT and DPPC lipid extraction have been investigated, it is expected that such a drug delivery system has the ability to penetrate the membrane, even at low velocities. We hope that the results obtained in this work shed light on the behavior of intracellular and targeted drug delivery systems.

Acknowledgments This work was partly supported financially by the Iran Nanotechnology Initiative Council and by provision of computer facilities for high-performance computing from the Research Center of Amirkabir University of Technology, for which the authors are grateful.

References

Allen MP, Tildesley DJ (1987) Computer simulation of liquids. Oxford University Press, New York

Berendsen HJC, Postma JPM, van Gunsteren WF, Hermans J (1981) Interaction models for water in relation to protein hydration. In: Pullman B (ed) Intermolecular forces. Reidel, Dordrecht, pp 331–342

Bianco A, Kostarelos K, Prato M (2005) Applications of carbon nanotubes in drug delivery. Curr Opin Chem Biol 9:674–679

Chaban VV, Savchenko TI, Kovalenko SM, Prezhdo OV (2010) Heat-driven release of a drug molecule from carbon nanotubes: a molecular dynamics study. J Phys Chem B 114:13481–13486

Cherukuri P, Bachilo SM, Litovsky SH, Weisman RB (2004) Near-infrared fluorescence microscopy of single-walled carbon nanotubes in phagocytic cells. J Am Chem Soc 126:15638–15639

Darden T, York D, Pedersen L (1993) Particle mesh Ewald: an N–log(N) method for Ewald sums in large systems. J Chem Phys 98:10089–10092

DeLano WL (ed) (2002) The PyMOL molecular graphics system. DeLano Scientific, San Carlos

DeVane R, Klein ML, Chiu C, Nielsen SO, Shinoda W, Moore PB (2008) Coarse-grained potential models for phenyl-based molecules: I. Parameterization using experimental data. J Phys Chem B 114:6386–6393

Dhar S, Liu Z, Thomale J, Dai H, Lippard SJ (2008) Targeted single-wall carbon nanotube-mediated Pt(IV) prodrug delivery using folate as a homing device. J Am Chem Soc 130:11467–11476

Domanski J, Stansfeld P, Sansom MSP, Beckstein O (2010) Lipidbook: a public repository for force field parameters used in membrane simulations. J Membr Biol 236:255–258

Egberts E, Marrink SJ, Berendsen HJC (1994) Molecular dynamics simulation of a phospholipid membrane. Eur Biophys J 22:423–436

Faraji AH, Wipf P (2009) Nanoparticles in cellular drug delivery. Bioorg Med Chem 17:2950–2962

Farokhzad OC, Langer R (2009) Impact of nanotechnology on drug delivery. ACS Nano 3:16–20

Gangupomu VK, Capaldi FM (2011) Interactions of carbon nanotube with lipid bilayer membranes. J NanoMat 2011:6

Hari M, Loganzo F, Annable T et al (2006) Paclitaxel-resistant cells have a mutation in the paclitaxel-binding region of β-tubulin (Asp26Glu) and less stable microtubules. Mol Cancer Ther 5:270–278

Hess B, Bekker H, Berendsen HJC, Fraaije JGEM (1997) LINCS: a linear constraint solver for molecular simulations. J Comput Chem 18:1463–1472

Hess B, Kutzner C, van der Spoel D, Lindahl E (2008) GROMACS 4: algorithms for highly efficient, load-balanced, and scalable molecular simulation. J Chem Theory Comput 4:435–447

Hilder TA, Hill JM (2008a) Carbon nanotubes as drug delivery nanocapsules. Curr Appl Phys 8:258–261

Hilder TA, Hill JM (2008b) Probability of encapsulation of paclitaxel and doxorubicin into carbon nanotubes. Micro Nano Lett 3:41–49

Hoover WG (1985) Canonical dynamics: equilibrium phase-space distributions. Phys Rev A 31:1695–1697

Hughes GA (2005) Nanostructure-mediated drug delivery. Nanomed Nanotechnol Biol Med 1:22–30

Humphrey W, Dalke A, Schulten K (1996) VMD: visual molecular dynamics. J Mol Graph 14:33–38

Izrailev S, Stepaniants S, Isralewitz B, Kosztin D, Lu H, Molnar F, Wriggers W, Schulten K (1997) Steered molecular dynamics. In: Deuflhard P, Hermans J, Leimkuhler B, Mark AE, Reich S, Skeel RD (eds) Computational molecular dynamics: challenges, methods, ideas. Springer, Berlin, pp 39–65

Jana AK, Jose JC, Sengupta N (2013) Critical roles of key domains in complete adsorption of Ab peptide on single-walled carbon nanotubes: insights with point mutations and MD simulations. Phys Chem Chem Phys 15:837–844

Johnson RR, Rego BJ, Johnson ATC, Klein ML (2009) Computational study of a nanobiosensor: a single-walled carbon nanotube functionalized with the coxsackie-adenovirus receptor. J Phys Chem B 113:11589–11593

Kandt C, Ash WL, Tieleman DP (2007) Setting up and running molecular dynamics simulations of membrane proteins. Methods 41:475–488

Kang Y, Wang Q, Liu Y, Wu T, Chen Q, Guan W (2008) Dynamic mechanism of collagen-like peptide encapsulated into carbon nanotubes. J Phys Chem B 112:4801–4807

Khodakovskaya M, Dervishi E, Mahmood M, Xu Y, Li Z, Watanabe F, Biris AS (2009) Carbon nanotubes are able to penetrate plant seed coat and dramatically affect seed germination and plant growth. ACS Nano 3:3221–3227

LaVan DA, McGuire T, Langer R (2003) Small-scale systems for in vivo drug delivery. Nat Biotechnol 21:1184–1191

Lay CL, Liu HQ, Tan HR, Liu Y (2010) Delivery of paclitaxel by physically loading onto poly(ethylene glycol) (PEG)-graft-carbon nanotubes for potent cancer therapeutics. Nanotechnology 21:10

Lee H (2013) Interparticle dispersion, membrane curvature, and penetration induced by single-walled carbon nanotubes wrapped with lipids and PEGylated lipids. J Phys Chem B 117:1337–1344

Liu Z, Chen K, Davis C, Sherlock S, Cao Q, Chen X, Dai H (2008) Drug delivery with carbon nanotubes for in vivo cancer treatment. Cancer Res 68:6652–6660

Martin CR, Kohli P (2003) Emerging field of nanotube biotechnology. Nat Rev Drug Discov 2:29–37

Nagle JF (1993) Area: lipid of bilayers from NMR. Biophys J 64:1476–1481

Ochekpe NA, Olorunfemi PO, Ngwuluka NC (2009) Nanotechnology and drug delivery part 2: nanostructures for drug delivery. Trop J Pharm Res 8:275–287

Panczyk T, Warzocha TP (2009) Monte Carlo study of the properties of a carbon nanotube functionalized by magnetic nanoparticles. J Phys Chem C 113:19155–19160

Panczyk T, Warzocha P, Camp PJ (2010) A magnetically controlled molecular nanocontainer as a drug delivery system: the effects of carbon nanotube and magnetic nanoparticle parameters from Monte Carlo simulations. J Phys Chem C 114:21299–21308

Pantaotto D, Briand J-P, Prato M, Bianco A (2004) Translocation of bioactive peptides across cell membrane by carbon nanotubes. Chem Commun 1:16–17

Parrinello M, Rahman A (1980) Crystal structures and pair potential: a molecular-dynamics study. Phys Rev Lett 45:1196–1199

Porter AE, Gass M, Muller K, Skepper JN, Midgley PA, Welland M (2007) Direct imaging of single-walled carbon nanotubes in cells. Nat Nanotechnol 2:713–717

Schuttelkopf AW, van Aalten MF (2004) PRODRG: a tool for high-throughput crystallography of protein–ligand complexes. Acta Cryst 60:1355–1363

Shepherd CM, Schaus KA, Vogel HJ, Juffer AH (2001) Molecular dynamics study of peptide-bilayer adsorption. Biophys J 80:579–596

Shi X, Kong Y, Gao H (2008) Coarse grained molecular dynamics and theoretical studies of carbon nanotubes entering cell membrane. Acta Mech Sin 24:161–169

Shuai Z, Kai Y, Zhuang L (2010) Carbon nanotubes for in vivo cancer nanotechnology. Sci China Chem 53:2217–2225

Snyder JP, Nettles JH, Cornett B, Downing KH, Nogales E (2001) The binding conformation of Taxol in beta-tubulin: a model based on electron crystallographic density. Proc Natl Acad Sci USA 98:5312–5316

Su Z, Zhu S, Donkor AD, Tzoganakis C, Honek JF (2011) Controllable delivery of small-molecule compounds to targeted cells utilizing carbon nanotubes. J Am Chem Soc 133:6874–6877

Sung J, Barone PW, Kong H, Strano MS (2009) Sequential delivery of dexamethasone and VEGF to control local tissue response for carbon nanotube fluorescence based micro-capillary implantable sensors. Biomaterials 30:622–631

Surendiran A, Sandhiya S, Pradhan SC, Adithan A (2009) Novel applications of nanotechnology in medicine. Indian J Med Res 130:689–701

Sutmann G (2002) Classical molecular dynamics. NIC Series 10:211–254

Tieleman DP, Marrink SJ, Berendsen HJC (1997) A computer perspective of membranes: molecular dynamics studies of lipid bilayer systems. Biochim Biophys Acta 1331:235–370

Ulbrich W, Lamprecht A (2010) Targeted drug-delivery approaches by nanoparticulate carriers in the therapy of inflammatory diseases. J R Soc Interface 7:S55–S66

van Gunsteren WF, Billeter SR, Ebbesen TW, Hunenberger PH, Kruger P, Mark AE, Scott WRP, Tironi IG (1996) Biomolecular simulation: the GROMOS96 manual and user guide. Swiss Federal Institute of Technology, Zürich

Wallace EJ, Sansom MSP (2008) Blocking of carbon nanotube based nanoinjectors by lipids: a simulation study. Nano Lett 8:2751–2756

Walther JH, Jaffe R, Halicioglu T, Koumoutsakos P (2001) Carbon nanotubes in water: structural characteristics and energetics. J Phys Chem B 105:9980–9987

Zuo G, Huang Q, Wei G, Zhou R, Fang H (2010) Plugging into proteins: poisoning protein function by a hydrophobic nanoparticle. ACS Nano 4:7508–7514

Zuo G, Gu W, Fang H, Zhou R (2011) Carbon nanotube wins the competitive binding over proline-rich motif ligand on SH3 domain. J Phys Chem C 115:12322–12328